

# Synthesis and characterization of new bimetallic transition metal oxynitrides: $M_I-M_{II}-O-N$ ( $M_I, M_{II} = V, Mo, W$ and Nb)

C. C. YU, S. T. OYAMA

*Department of Chemical Engineering, Virginia Tech. Blacksburg, VA 24061 USA*

A new class of materials,  $M_I-M_{II}-O-N$  (where  $M_I, M_{II} = V, Mo, W$ , and Nb), has been synthesized by nitriding bimetallic oxide precursors with ammonia gas *via* a temperature programmed reaction. The oxide precursors are prepared by conventional solid state reaction between two appropriate monometallic oxides. The synthesis of the oxynitrides involves passing  $NH_3$  gas over the oxide precursors at a flow rate of  $6.80 \times 10^2 \mu\text{mol s}^{-1}$  ( $1000 \text{ cm}^3 \text{ min}^{-1}$ ), and raising the temperature at a rate of  $8.3 \times 10^{-2} \text{ K s}^{-1}$  ( $5 \text{ K min}^{-1}$ ) to a final temperature which is held constant for a short period of time. The oxynitrides thus obtained are pyrophoric and need to be passivated before exposing them to air. All these new bimetallic oxynitrides have a face centered cubic (f.c.c.) metal arrangement and high values of surface area. Their surface activity is assessed from their ability to chemisorb CO.

## 1. Introduction

Nitride formation is common to most transition elements. Many compositional and structural forms exist, with many transition elements forming several different nitride phases. In many of these compounds, nitrogen atoms occupy interstitial lattice sites because they are smaller than the metal atoms [1]. For this reason, they are often referred to as interstitial compounds. Transition metal nitrides are of technological importance. They have extreme hardness, excellent corrosion resistance and high temperature stability and have thus found applications as cutting tools, wear-resistant parts and hard coatings [2–8]. They also possess electronic and magnetic properties that make them useful as electronic and magnetic components [9–18] and as superconductors [19–25]. In the 1980s, transition metal nitrides attracted considerable attention as catalysts due to their similarity to the noble Group VIII metals (Pt, Pd, Rh, etc.) in activity, and in some cases, their superior selectivity, stability and resistance to poisoning [26–32].

Although monometallic nitrides have been the object of considerable studies [1, 33], bimetallic nitrides have attracted only limited attention [5, 34, 35]. Similarly, the literature on oxynitrides has been scarce. It has been known that oxygen atoms can substitute nitrogen atoms in monometallic nitrides due to the similarity in their radius [36, 37]. However, recent years have seen considerable progress in the synthesis of bimetallic nitrides and oxynitrides [5, 35, 38]. Examples are compounds like  $LiMoN_2$  [39],  $Li_3FeN_2$  [40],  $CaCrN_3$  [41], and  $LaTaON_2$  [42], which are formed from combinations of transition metals with alkali, alkaline earth, and lanthanide elements. A number of bimetallic compounds with only

transition metals also have been reported. Among these are  $NbCrN$  [43],  $CuWN_2$  [44],  $FeWN_2$  [45],  $Fe_3Mo_3N$  and  $Ni_3Mo_3N$  [46]. The oxynitrides prepared here are related to  $CuWN_2$  and  $FeWN_2$  in that they have high concentrations of the non-metal elements, but have cubic instead of hexagonal structure.

The bonding in bimetallic nitrides and oxynitrides containing electropositive elements is mostly ionic, but can be partly covalent or metallic. For example, in the  $Ca_3MN$  series, the compounds can be insulators ( $M = As$  or  $P$ ), semiconductors ( $M = Bi, Sb$ ) or conductors ( $M = Pb, Sn, Ge$ ) depending on the filling of the  $sp$  bands [47]. Their ionic character and their limiting compositions can be described by the normal rules of valency ( $-2$  for O,  $-3$  for N) [45]. This is not the case for the compounds of exclusively transition metals, which are mostly metallic in nature. As with the binary transition metal compounds, cohesive strengths are dominated by metal–metal bonding [48]. In many of the compounds, the N and O atoms are found in interstitial lattice positions in between the metal atoms. For this reason their phases can exist over broad composition ranges with appreciable vacancy concentrations (both metal and non-metal) and their physical properties are quite sensitive to composition. For example, titanium oxide exists between the limits  $TiO_{0.64}$  (36% O vacancies) and  $TiO_{1.26}$  (21% Ti vacancies) [49], while titanium nitride forms between the limits  $TiN_{0.42}$  (58% N vacancies)– $TiN_{1.16}$  (14% Ti vacancies) [50]. At the stoichiometric composition TiO has 15% vacancies of each element and TiN has 4% vacancies of each. Changes in valence electron density are probably a major cause of the composition sensitivity of the properties. The exchange of nitrogen by oxygen, and at the same time,

the partial substitution of one transition metal by another are expected to substantially alter the properties of the compounds.

The new bimetallic oxynitrides reported here were prepared by temperature programmed reaction (TPR), a technique developed in the last decade which produces nitrides with high specific surface areas [29, 51]. The current TPR approach involves placing a bimetallic oxide precursor in a flowing ammonia stream while raising the temperature in a controlled manner. The bimetallic oxide precursors were prepared by the solid state reaction of two monometallic oxides.

## 2. Experimental procedure

### 2.1. Materials

Materials used in the current investigation were molybdenum (VI) oxide ( $\text{MoO}_3$ , 99.95%), tungsten (VI) oxide ( $\text{WO}_3$ , 99.8%), vanadium (V) oxide ( $\text{V}_2\text{O}_5$ , 99.9%), and niobium (V) oxide ( $\text{Nb}_2\text{O}_5$ , 99.9%). The gases employed were  $\text{NH}_3$  (99.99%), He (99.999%), CO (99.97%) and 0.5%  $\text{O}_2/\text{He}$ .

### 2.2. Synthesis

Bimetallic oxide precursors were prepared by the solid state reaction of two monometallic oxides. The two monometallic oxides, at a pre-chosen metal ratio (Table I), were first ground together using a mortar and pestle with added ethanol to achieve better dispersion. They were then partially dried, and pressed at about 55.2 MPa in a 1.27 cm diameter hard steel die. Since the remaining ethanol in the mixture facilitated compacting, no binder was needed for pellet pressing. The oxide pellets were subsequently fired at high temperature for 6 h and were finally cooled to room temperature, and pulverized in preparation for the nitriding step. The preparation conditions for the bimetallic oxides, including starting materials used, metal ratios chosen, and final firing temperatures, are summarized in Table I.

Bimetallic oxynitrides were prepared by the temperature programmed reaction of the bimetallic oxides with ammonia. The bimetallic oxide powders synthesized, as described above, were transferred to a quartz reactor, which was placed inside a tubular resistance furnace (550 W) controlled by a temperature programmer. An ammonia gas stream was passed through the oxide powders at a flow rate of  $6.80 \times 10^2 \mu\text{mol s}^{-1}$  ( $1000 \text{ cm}^3 \text{ min}^{-1}$ ). The temperature was increased at a linear rate of  $8.3 \times 10^{-2} \text{ K s}^{-1}$  ( $5 \text{ K min}^{-1}$ ) to a final temperature

( $T_f$ ) which was held for a period of time ( $t_{\text{hold}}$ ). The furnace was then removed to quench the samples and the flow of ammonia gas was switched to helium and maintained during the cooling process (15 min). After cooling, the pure He gas was switched to a gas mixture containing 0.5%  $\text{O}_2$  in He at a flow rate of  $24 \mu\text{mol s}^{-1}$  ( $35 \text{ cm}^3 \text{ min}^{-1}$ ) to passivate the samples. The time of passivation was set to 3 h per gram of starting bimetallic oxide used. The synthesis conditions of bimetallic oxynitrides,  $T_{\text{max}}$  and  $t_{\text{hold}}$ , are listed in Table II.

### 2.3. Characterization

X-ray diffraction (XRD) analysis of both bimetallic oxides and bimetallic oxynitrides was carried out using a powder diffractometer with a  $\text{CuK}_\alpha$  monochromatized radiation source, operated at 40 kV and 30 mA. The oxynitride samples were also characterized by inductively coupled plasma (ICP) elemental analysis, CO chemisorption, and  $\text{N}_2$  physisorption.

For CO chemisorption measurements, the passivated oxynitrides were first reactivated at 738 K for 2 h under a reductive gas stream containing 10%  $\text{H}_2$ -90% He. At the end of the reactivation process, the  $\text{H}_2/\text{He}$  gas mixture was switched to pure He, and the samples were brought to room temperature. After cooling, pulses of CO gas were introduced through a sampling valve with the He carrier gas stream passing over the samples. The effluent gas stream was sampled into a mass spectrometer chamber through a variable leak valve. A computer recorded the mass signals of the effluent gas and the sample temperatures through a RS232 interface. The total uptake was calculated by referring the areas under the CO mass signal (28) peaks to the calibrated quantity of  $12.02 \mu\text{mol CO}$  for a single peak.

Surface areas were determined by a similar flow technique using a 30%  $\text{N}_2$  in He gas mixture passed over the samples maintained at liquid nitrogen

TABLE II Synthesis conditions for bimetallic oxynitrides ( $M_I$ - $M_{II}$ -O-N)

System ( $M_I$ - $M_{II}$ -O-N)	Metal ratio ( $M_I:M_{II}$ )	Final temperature ( $T_f$ ) (K)	Time hold at $T_f$ ( $t_{\text{hold}}$ ) (min)
V-Mo-O-N	2:1	1037	30
Nb-Mo-O-N	2:3	1063	20
V-W-O-N	1:1	1009	110
Mo-W-O-N	1:1	991	20
Nb-W-O-N	2:3	1113	24

TABLE I Preparation conditions for bimetallic oxides ( $M_I$ - $M_{II}$ -O)

System ( $M_I$ - $M_{II}$ -O)	Starting materials	Metal ratio ( $M_I:M_{II}$ )	Firing temperature ( $T_{\text{max}}$ ) (K)	Time hold at $T_{\text{max}}$ (h)
V-Mo-O	$\text{V}_2\text{O}_5$ - $\text{MoO}_3$	2:1	948	6
Nb-Mo-O	$\text{Nb}_2\text{O}_5$ - $\text{MoO}_3$	2:3	1058	6
V-W-O	$\text{V}_2\text{O}_5$ - $\text{WO}_3$	1:1	1323	6
Mo-W-O	$\text{MoO}_3$ - $\text{WO}_3$	1:1	1058	6
Nb-W-O	$\text{Nb}_2\text{O}_5$ - $\text{WO}_3$	2:3	1323	6

temperature. The amount of physisorbed  $N_2$  was obtained by comparing the area of the desorption peaks to the area of calibrated  $N_2$  pulses containing  $37.95 \mu\text{mol } N_2/\text{pulse}$ . The surface area was then calculated from the single point Brunauer–Emmett–Teller (BET) equation.

### 3. Results and discussion

#### 3.1. Crystalline phases

Fig. 1(a–e) shows the XRD patterns of the ternary oxides after solid state reaction. For comparison, the XRD patterns of the starting monoxides are shown in Fig. 2(a–d). The prominent features of each product's XRD pattern, i.e. peak position and intensity, do not match those of the parent oxides, nor their reduced forms. The results indicate that at least the major phases of the products are true bimetallic oxides, instead of mechanical mixtures of the starting oxides.

Fig. 3(a–e) shows the XRD patterns of the oxynitrides prepared by the temperature programmed reaction. The XRD peak d-spacing and their indexing are listed in Table III. The results indicate, interestingly, that all the oxynitrides thus synthesized have face centered cubic (f.c.c.) metal arrangements. Furthermore, the broadening of the XRD peaks indicates that these oxynitrides have very small crystallite sizes, which in turn suggests high surface areas in these materials. The small sharp feature in the Mo–W–O–N sample (Fig. 3(d)) is due to a small amount of unreacted oxide.

The five-peak pattern (four are visible in the scale presented) of the X-ray diffraction spectra (Fig. 3) of the oxynitrides is consistent with the rock salt crystal structure (space group  $Fm\bar{3}m$ ) where the metal atoms are placed in a f.c.c. arrangement and N or O fill

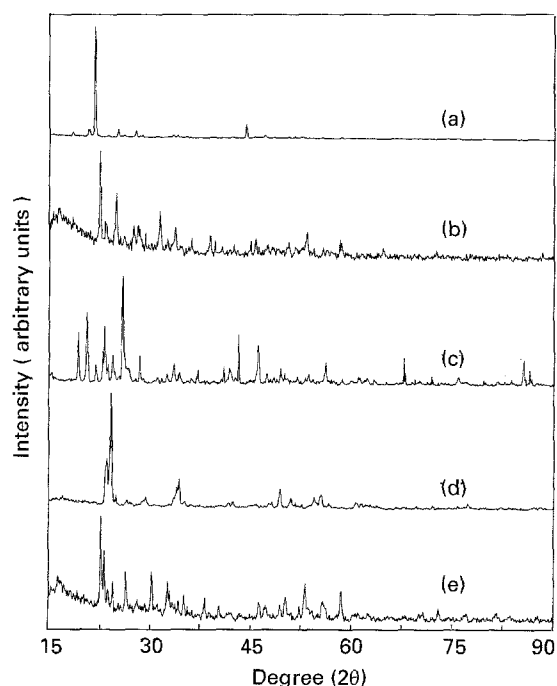


Figure 1 XRD patterns of bimetallic oxides ( $M_I-M_{II}-O$ ). (a) V–Mo–O; (b) Nb–Mo–O; (c) V–W–O; (d) Mo–W–O; (e) Nb–W–O.

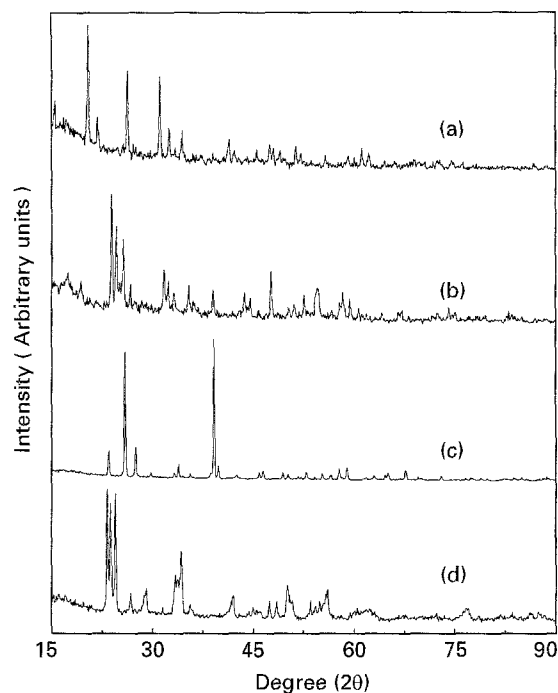


Figure 2 XRD patterns of parent monometallic oxides. (a)  $V_2O_5$ ; (b)  $Nb_2O_5$ ; (c)  $MoO_3$ ; (d)  $WO_3$

octahedral interstitial positions [52]. The fcc metallic arrangement is also found in molybdenum nitride ( $Mo_2N$ ) or oxycarbide ( $MoO_xC_y$ ), but these are monometallic compounds and the non-metallic elements fill only half of the available octahedral holes [53]. For bimetallic nitrides and oxynitrides this type of structure is unreported, as indicated in a recent comprehensive review [54]. Thus, the materials probably are a new composition of matter.

#### 3.2. Surface characteristics

Chemisorption is perhaps the most widely used method for assessing the surface activity of a material. In the currently employed pulse technique, a precise amount ( $12.02 \mu\text{mol}$ ) of CO gas was injected onto a He carrier gas stream which flowed over the reduced oxynitride. The unadsorbed adsorbate gas (CO) was detected by the mass spectrometer and recorded in the form of peaks. Pulses were repeated until successive peaks showed the same area, and the adsorption was complete. The difference between the area of these peaks and the previous peaks gave the irreversible uptake of the adsorbate gas by the material and was calculated by the equation

$$n_{\text{ads}} = \sum n_{i\text{inj}} [1 - (A_i/A_s)] \quad (1)$$

where  $n_{\text{ads}}$  is the total amount of gas adsorbed,  $n_{i\text{inj}}$  is the volume of the injected pulse ( $= 12.02 \mu\text{mol}$ ),  $A_i$  is the area of the  $i^{\text{th}}$  peak and  $A_s$  is the area of the peak at saturation. Fig. 4(a) shows the mass signal trace ( $M = 28$ , CO) in the pulse CO chemisorption measurement of the Mo–W–O–N sample. Note the very small initial CO peak due to the almost total uptake of the first dose by the sample.

Fig. 4(b) is the mass signal trace ( $M = 28$ ,  $N_2$ ) in a single-point BET experiment of the Mo–W–O–N

TABLE III XRD peak d-spacing and indexing of bimetallic oxynitrides  $M_I-M_{II}-O-N$ 

d-spacing					Indexing
V-Mo-O-N	Nb-Mo-O-N	V-W-O-N	Mo-W-O-N	Nb-W-O-N	
2.38	2.45	2.39	2.40	2.42	111
2.06	2.11	2.06	2.07	2.09	200
1.46	1.50	1.46	1.47	1.48	220
1.24	1.27	1.25	1.25	1.26	311
1.19	1.22	1.20	-	-	222

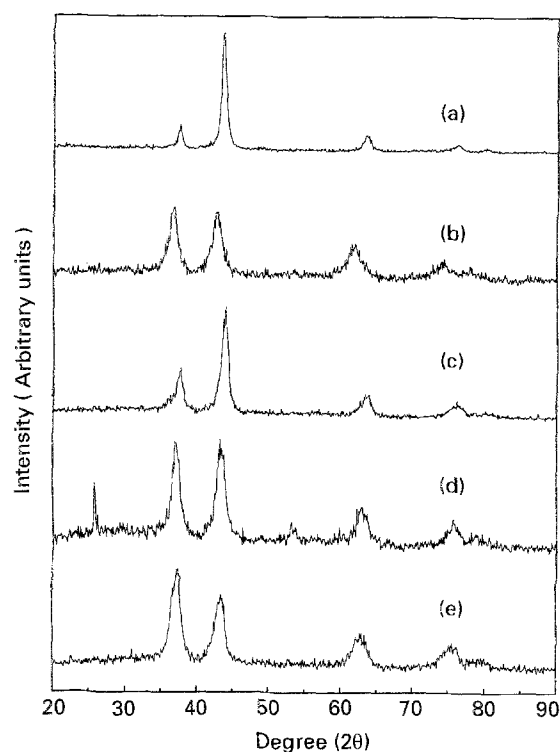


Figure 3 XRD patterns of bimetallic oxynitrides ( $M_I-M_{II}-O-N$ ). (a) V-Mo-O-N; (b) Nb-Mo-O-N; (c) V-W-O-N; (d) Mo-W-O-N; (e) Nb-W-O-N.

sample. The measurement was carried out by flowing a 30%  $N_2$  in He gas mixture over the sample. The small sharp peaks at the beginning and end of the experiment are  $N_2$  calibration peaks ( $A_c$ ). Adsorption commenced when the sample cell was immersed in liquid nitrogen, and the mass spectrometer recorded the decrease in  $N_2$  concentration in the gas stream as a negative peak ( $A_{ads}$ ). Upon completion of adsorption, the  $N_2$  signal returned to its original value and when the liquid nitrogen was removed, desorption occurred and was recorded as a positive peak ( $A_{des}$ ). The volume of  $N_2$  adsorbed or desorbed was calculated against the area of injected calibration pulses ( $A_c$ ). The surface area of the sample was determined by the equation

$$S_g = n_{des} N_A A (1 - P/P_0) / Wt \quad (2)$$

where  $S_g$  is the specific surface area in  $m^2 g^{-1}$ ,  $n_{des}$  is the amount of nitrogen desorbed ( $\mu mol$ ),  $N_A$  is Avogadro's number,  $A$  is the area of one  $N_2$  molecule ( $16 \times 10^{-20} m^2$ ),  $P/P_0$  is the partial pressure of  $N_2$  in the mixture gas and  $Wt$  is the weight of the sample (g).

Table IV summarizes the calculated CO uptake, surface area and the active site density of these oxy-

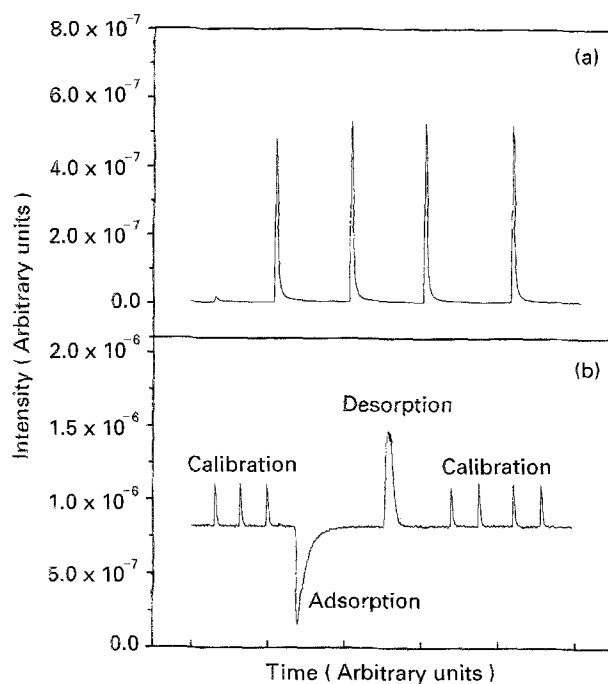


Figure 4 Mass signal ( $M = 28$ ) trace of (a) CO chemisorption measurement on Mo-W-O-N; and (b)  $N_2$  physisorption measurement on Mo-W-O-N.

nitrides. All the samples have high surface area, from  $62 m^2 g^{-1}$  up to  $121 m^2 g^{-1}$ , consistent with the observed XRD peak broadening. The CO uptakes range from  $9.67 \mu mol g^{-1}$  to  $167 \mu mol g^{-1}$ .

The chemisorption of CO can be used to titrate accessible surface metal atoms in the materials [55, 56]. Normally for metals and metal alloys the surface site density is  $\sim 1 \times 10^{15} cm^{-2}$  [57]. The values obtained in this study are in the range  $0.01-0.10 \times 10^{15} cm^{-2}$ , indicating that 1-10% of the metal atoms are chemisorbing CO. These values are consistent with previously reported quantities for carbides and nitrides [55, 58]. It is likely that the initial 2-h reactivation at 738 K does not remove all the N and O species from the surface, which thus block CO chemisorption [59-61]. This may be exacerbated by replenishment of N and O from the bulk. These species are known to be mobile in the sub-surface at these temperatures [62].

### 3.3. Bulk characteristics

Table V lists the elemental analysis data of the bimetallic oxynitrides prepared by the temperature

TABLE IV Characteristics of bimetallic oxynitrides ( $M_I-M_{II}-O-N$ )

Compounds	CO uptake ( $\mu\text{mol g}^{-1}$ )	Surface area ( $S_g \text{ m}^2 \text{ g}^{-1}$ )	Site density ( $\times 10^{15} \text{ cm}^{-2}$ )	Particle size <sup>a</sup> $D_p$ (nm)	Crystalline size <sup>b</sup> $D_c$ (nm)
V-Mo-O-N	167	74	0.14	7.9	11
Nb-Mo-O-N	11.2	121	0.0056	4.9	5.3
V-W-O-N	9.67	62	0.0094	5.1	6.7
Mo-W-O-N	59.2	118	0.030	5.0	6.5
Nb-W-O-N	32.7	81	0.024	3.9	5.2

$$^a D_p = 6(S_g \rho) \rho_{\text{Mo}} = 10.2 \text{ g cm}^{-2} \rho_w = 18.9 \text{ g cm}^{-3}.$$

$$D_c = K/\lambda \beta \cos \theta \beta^2 = B^2 - b^2 = B^2 - 0.1^2.$$

TABLE V Molar composition of bimetallic oxynitrides ( $M_I-M_{II}-O-N$ ) (from elemental analysis)

Compounds	V	Nb	Mo	W	O	N
V-Mo-O-N	2.0	-	1.0	-	1.7	2.4
Nb-Mo-O-N	-	2.0	2.6	-	3.0	4.2
V-W-O-N	1.0	-	-	1.4	2.7	2.5
Mo-W-O-N	-	-	1.0	1.0	2.4	2.1
Nb-W-O-N	-	2.0	-	2.8	4.5	5.1

programmed reaction. For Nb-Mo and V-W systems, the metal ratio in the oxynitrides (Nb:Mo = 2.0:2.6 and V:W = 1.0:1.4) deviates from that of the starting conditions (Nb:Mo = 2.0:3.0 and V:W = 1.0:1.0). This is probably caused by the sublimation of MoO<sub>3</sub> and V<sub>2</sub>O<sub>5</sub> during the bimetallic oxide synthesis.

The unusually broad diffraction peaks indicate a finely divided substance. Indeed, the crystallite size  $D_c$ , calculated by the Scherrer equation [63] suggests dimensions of the order 3 to 11 nm (Table III). This is confirmed by the high values of the surface area,  $S_g$ . The particle size can be calculated from the equation

$$D_p = 6/(S_g \rho) \quad [64] \quad (3)$$

where  $\rho$  is taken to be 10.24 g cm<sup>-3</sup> for Mo oxynitride compounds and 18.9 g cm<sup>-3</sup> for W oxynitride compounds, assuming perfect rock salt structures for these compounds. There is good agreement between  $D_p$  and  $D_c$ , indicating that the particles are not polycrystalline aggregates.

#### 4. Conclusions

A new class of materials,  $M_I-M_{II}-O-N$  (where  $M_I, M_{II} = \text{V, Mo, W and Nb}$ ), have been synthesized by a temperature programmed reaction process. All these new bimetallic oxynitrides adopt a f.c.c. metal arrangement. They are surface active (CO chemisorption ranging from 9.67  $\mu\text{mol g}^{-1}$  to 167  $\mu\text{mol g}^{-1}$ ), and have high surface area (62 ~ 121  $\text{m}^2 \text{ g}^{-1}$ ). Their surface activity combined with high surface area make them very interesting materials with potential application as catalysts and ceramic precursors. The oxynitride synthesis temperatures are moderate (< 1120 K), the cycles are short (moderate heating rate and holding times), and the parameters are easy to control. The oxide precursors used for the oxynitride synthesis are prepared by conventional solid state reaction using common starting materials.

#### Acknowledgements

This paper was written with support from Akzo Nobel and the US Department of Energy under the Advanced Coal Research at US Universities Program, Grant DE-PS22-95PC95200.

#### References

1. L. E. TOTH, "Transition metal carbides and nitrides", (Academic Press, New York, 1971).
2. P. SCHWARTZKOPF and R. KIEFFER in "Refractory hard metals", (MacMillan, New York, 1953).
3. G.V. SAMSONOV, in "Refractory transition metal compounds; high temperature cermets", (Academic Press, New York and London, 1964).
4. M. MOLARIUS, A. S. KORHONEN and E. O. RISTOLAINEN, *J. Vac. Sci. Technol.* **A3** (1985) 2419.
5. F. J. DISALVO, *Science* **247** (1990) 649.
6. R. M. FIX, R. G. GORDON and D. M. HOFFMAN, *Chem. Mater.* **2** (1990) 235.
7. S. DRESSLER, *Indust. Heating* **October** 1992, p. 38.
8. S. T. OYAMA, *J. Solid State Chem.* **96** (1992) 442.
9. G. W. WILNER and J.A. BERGER, *J. Met.* **7** (1955) 360.
10. M. MEKATA, *J. Phys. Soc. Japn.* **17** (1962) 796.
11. T. K. TIM and M. TAKAHASHI, *Appl. Phys. Lett.* **20** (1972) 492.
12. K. TAGAWA, E. KITA and A. TASAKI, *Japn. J. Appl. Phys.* **21** (1982) 1596.
13. W. J. GARCEAU and G. K. HERB, *Thin Solid Films* **60** (1979) 237.
14. C. ERNSBERGER, A. MILLER and D. BANKS, *J. Vac. Sci. Technol.* **A3** (1985) 2303.
15. M. WITTMER and H. MELCHIOR, *Thin Solid Films* **93** (1982) 397.
16. M. WITTMER, *J. Vac. Sci. Technol.* **A3** (1985) 1979.
17. N. KUMAR, J. T. MCGINN, K. POURREZAEI, B. LEE and C. DOUGLAS, *Ibid.* **A6** (1988) 1602.
18. Y. OTANI, D. P. F. HURLEY, H. SUN and J. M. D. COEY, *J. Appl. Phys.* **69** (1991) 5584.
19. E. K. STORMS, *LAMS-2674* (Part II) (1962).
20. T. H. COURTNEY, J. REINTJES and J. WULFF, *J. Appl. Phys.* **36** (1965) 660.
21. L. E. TOTH, C. P. WANG and C. M. YEN, *Acta Metall.* **14** (1966) 1403.
22. Y. M. SHY, L. E. TOTH and R. SOMASUNDARAM, *J. Appl. Phys.* **44** (1973) 5539.
23. L. E. TOTH and C. M. YEN, *J. Phys. Chem. Solids* **27** (1966) 1815.
24. C. M. YEN, L. E. TOTH and Y. M. SHY, *J. Appl. Phys.* **38** (1967) 2268.
25. H. BELL, Y. M. SHY, D. E. ANDERSON and L. E. TOTH, *Ibid.* **39** (1968) 2797.
26. M. SAITO and R. B. ANDERSON, *J. Catal.* **63** (1980) 438.
27. M. BOUDART, S. T. OYAMA and L. LECLERCQ, in Proceedings of the 7th International Congress Catal., Tokyo, 1980, edited by T. SEIYAMA and K. TANABE, Vol. 1, (Kodansha, 1980) p. 578.

28. S. T. OYAMA and G. L. HALLER, *Catalysis, Spec. Period. Rep.* **5** (1981) 333.
29. L. VOLPE and M. BOUDART, *J. Solid State Chem.* **59** (1985) 332.
30. D. J. SAJKOWSKI and S. T. OYAMA, Preprints, Petroleum Chemistry Division, Symposium on "The chemistry of W/Mo catalysis", 199th ACS National Meeting, Boston, Massachusetts, April 22-27, 1990.
31. E. J. MARKEL, and J. W. VAN ZEE, *J. Catal.* **126** (1990) 643.
32. S. T. OYAMA, *Catalysis Today* **15** (1992) 179.
33. R. JUZA, in "Advances in inorganic chemistry and radiochemistry", edited by H.J. EMELEUS and A. G. SHARPE (Academic Press, New York and London, 1966) Vol. 9, p. 81.
34. D. S. BEM, and H. C. ZUR LOYE, *J. Solid State Chem.* **104** (1993) 467.
35. T. YAMAMOTO, S. KIKKAWA, and F. KANAMARU, *Solid State Ionics* **63-65** (1993) 148.
36. R. KIESSLING, and L. PETERSON, *Acta Metall.* **2** (1954) 675.
37. N. SCHÖNBERG, *Acta Chem. Scand.* **8** (1954) 208.
38. S. H. ELDER, F. J. DISALVO, L. TOPOR and A. NAVROTSKY, *Chem. Mater.* **5** (1993) 1545.
39. S. H. ELDER, L. H. DOERRER, F. J. DISALVO, J. B. PARISE, D. GUYOMARD and J. M. TARASCON, *Ibid.* **4** (1992) 928.
40. A. GUDAT, R. KNIEP, A. RABENAU, W. BRONGER and U. RUSCHEWITZ, *J. Less-Common Metals* **161** (1990) 31.
41. D. A. VENNOS, M. E. BADDING and F. J. DISALVO, *Inorg. Chem.* **29** (1990) 4059.
42. R. MARCHAND, F. PORS and Y. LAURENT, *Ann. Chim. Fr.* **16** (1991) 553.
43. P. VERDIER, P. L'HARIDON, M. MAUNAYE and R. MARCHAND, *Acta Cryst.* **B30** (1974) 226.
44. U. ZACHWIEJA and H. JACOBS, *Eur. J. Solid State Inorg. Chem.* **28** (1991) 1055.
45. D. S. BEM and H.-C. ZUR LOYE, *J. Solid State Chem.* **104** (1993) 467.
46. D. S. BEM, C. P. GIBSON and H.-C. ZUR LOYE, *Chem. Mater.* **5** (1993) 397.
47. M. Y. CHERN, D. A. VENNOS and F. J. DISALVO, *J. Solid State Chem.* **96** (1992) 415.
48. A. L. IVANOVSKII, D. L. NOVIKOV and V. A. GUBANOV, *Phys. Status Solidi* **141** (1987) 9.
49. B. G. HYDE and S. ANDERSON, "Inorganic crystal structures", (John Wiley & Sons, 1989) p. 11.
50. R. JUZA, in "Advances in inorganic chemistry and radiochemistry", Vol. 9, edited by H.J. Emeléus and A.G. Sharpe (Academic Press, New York, 1966) p. 81.
51. S. T. OYAMA, Ph.D. Dissertation, Stanford University, (1981).
52. B. G. HYDE and S. ANDERSSON, *Inorganic Crystal Structures* (Wiley, New York, 1989).
53. S. T. OYAMA, *J. Solid State Chem.* **96** (1992) 442.
54. N. E. BRESE and M. O'KEEFFE in "Structure and bonding", Vol. 79, "Complexes, Clusters and Crystal Chemistry" (Springer-Verlag, Berlin, 1992) p. 307.
55. J. S. LEE, S. LOCATELLI, S. T. OYAMA and M. BOUDART, *J. Catal.* **125** (1990) 157.
56. J. S. LEE, K. H. LEE and J. Y. LEE, *J. Phys. Chem.* **96** (1992) 362.
57. K. FOGER, in "Catalysis, science and technology", Vol 6, edited by J. R. Anderson and M. Boudart, (Springer-Verlag, Berlin, 1984) p. 227.
58. S. T. OYAMA, J. C. SCHLATTER, J. E. METCALFE, III and J. M. LAMBERT, Jr., *Ind. Eng. Chem. Res.* **27** (1988) 1639.
59. E. I. KO and R. J. MADIX, *Surf. Sci.* **100** (1980) L505.
60. *Idem, Ibid.* **109** (1981) 221.
61. G. S. RANHOTRA, A. T. BELL and J. A. REIMER, *J. Catal.* **108** (1987) 40.
62. K. J. LEARY, J. N. MICHAELS and A. M. STACY, *Ibid.* **101** (1986) 301.
63. P. SCHERRER, *Gött. Nachr.* **2** (1918) 98.
64. J. M. SMITH, "Chemical engineering kinetics", 3rd edition, (McGraw-Hill, New York, 1981) p. 328.

Received 16 September 1994  
and accepted 21 February 1995